Title	Electric Field Effects in Ultrathin YBa2Cu3O7-d Films (SOLID STATE CHEMISTRY-Artificial Lattice Compounds)
Author(s)	Bando, Yoshichika; Terashima, Takahito
Citation	ICR annual report (1997), 3: 18-19
Issue Date	1997-03
URL	http://hdl.handle.net/2433/65118
Right	
Type	Article
Textversion	publisher

Electric Field Effects in Ultrathin $YBa_2Cu_3O_{7-\delta}$ Films

Yoshichika Bando and Takahito Terashima

Charging effects on transport properties of ultrathin $YBa_2Cu_3O_{7-\delta}$ (YBCO) films are measured using FET-like junctions of YBCO in thickness ranging from 1 to 10 unit cell thicknesses (UCT). An electric(E-) field experiment without magnetic field finds that the changes of Kosterlitz-Thouless transition temperature is observed as a function of applied E-field. The changes of superconducting properties are linearly correlated to those of the normal resistance, namely, the induced areal carrier densities.

Keywords: High-T_C superconductivity/ $YBa_2Cu_3O_{7-\delta}$/ Ultrathin film/ Electric field effect

Electric (E-) field effects in superconductors have attracted much attentions from the interest in fundamental physics as well as the device applications. By using an E-field effect junction, we could examine an effect of the carrier density on superconductivity without any reconstruction of sample structure. The change of superconducting transition temperature T_C by E-field have observed for the first time for the thin films of conventional superconductors of Sn and In. Recent works on the E-field effects are mainly devoted to high temperature superconductors (HTSC) since the effects on superconductivity are expected to be large because of the low carrier density n and the short coherence length of HTSC. Here we will report the E-field effects in ultrathin $YBa_2Cu_3O_{7-\delta}$ (YBCO) films [1,2].

Figure 1 depicts the top view of a 3-terminal junction used in the E-field effect experiment. *C*-axis-oriented YBCO films with thicknesses from 1 to 10 unit-cell-thickness (UCT) were prepared onto a (100) surface of $SrTiO_3$(STO) by using an activated-reactive evaporation technique. A buffer layer of several UCT nonsuperconducting $PrBa_2Cu_3O_{7-\delta}$(PBCO) was first prepared onto a STO (100) substrate heated up to 680 ˚C, and then a YBCO film was grown onto the buffer layer of PBCO. After deposition of a 3 nm capping layer of STO on YBCO film, the film was cooled down to room temperature in an oxygen atmosphere of 0.01 MPa. After exposure to air, a masking plate was set up to open a window wider than the sample area of YBCO for STO deposition. A thick dielectric STO film (120 nm) was deposited onto the capping STO layer at 690˚C. Finally a gate electrode of thin Pt film (40nm) was prepared in a separate evaporator with a lead wire attached. The distribution of applied E-field in the YBCO film was uniform over the sample. An areal charge density ΔN induced in the junction area S ($0.51 cm^2$) of the YBCO film was evaluated by $\Delta N = CV_g/eS$ from an applied gate voltage V_g and a capacitance C that was almost independent of temperature T within an error of 20% in the temperature range of this experiment between 4K and 100K, where S is the surface area of the capacitor and e is the unit charge. The

SOLID STATE CHEMISTRY —Artificial Lattice Compounds—

Scope of research

Syntheses of oxide thin films by reactive evaporation and ceramics by solid state reaction and their characterizations are studied. The main subjects are: preparation and characterization of ultrathin films of high-T_c superconductors: investigation of growth mechanism of thin films by in situ reflection high-energy electron diffraction: phase diagram of Bi_2O_3-SrO-CaO-CuO system: growth and characterization of single crystals of Bi-Sr-Ca-Cu-O system: preparation and observation of dielectric properties of ferroelectric thin films: preparation and characterization of metallic and ferromagnetic $SrRuO_3$ thin films: scanning tunneling microscope observation of surface structures and electronic states of metallic oxide thin films

Prof
Bando, Yoshichika
(D Sc)

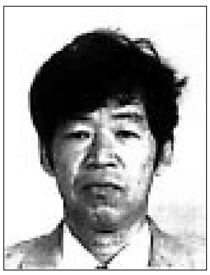

Instructor
IKEDA, Yasunori

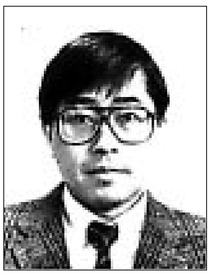

Instructor
TERASHIMA, Takahito
(D Sc)

Students:
IZUMI, Makoto (DC)
NIINAE, Toshinobu (DC)
NAKAZAWA, Kazuyuki (MC)
YAMADA, Takahiro (MC)
FURUBAYASHI, Yutaka (MC)
KAWANO, Katsuya

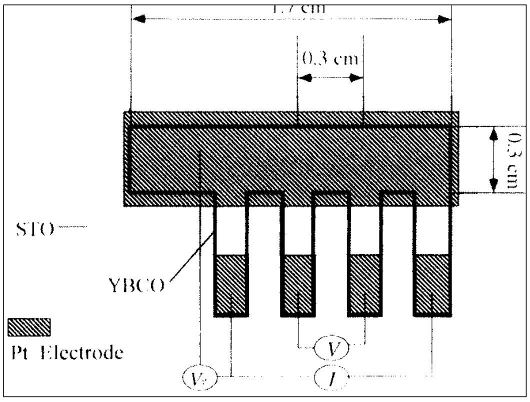

Figure 1. Top view of a FET-like junction.

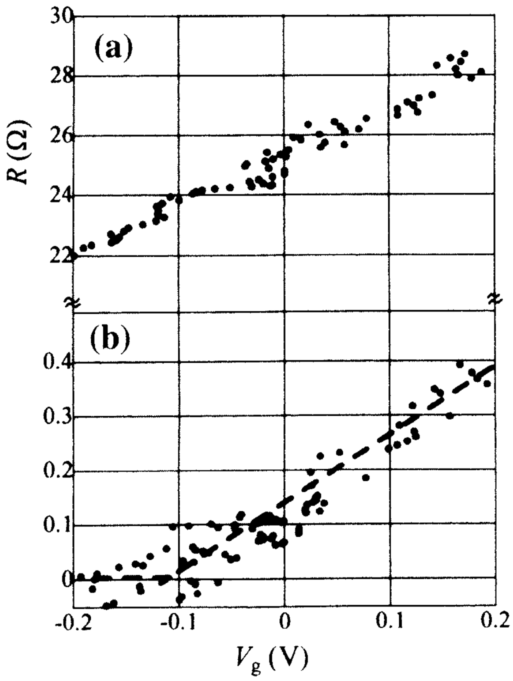

Figure 2. Change in R as a function of V_g for a 2UCT YBCO film at two representative fixed temperatures. (a) is for T = 45K and (b) for T = 35K, respectively.

dielectric constant of STO film was evaluated from the capacitance measurement as ε_e~2000 and the induced areal carrier density ΔN can be calculated via $\Delta N = \varepsilon_e \varepsilon_0 V_g / de$ = $9.22 \times 10^{13} V_g$(/cm^2) with d = 120nm, where ε_0 is the dielectric constant in vacuum.

E-field effects on resistance for 2 UCT (2.4nm)YBCO film are shown in Figs. 2(a) and (b) for representative fixed temperatures, that is, (a) is in the transition region of high resistance state at 45 K and (b) immediately above the onset temperature of R, respectively, where we applied a gate voltage to a Pt electrode. In Fig.2(a) , resistance R changes linearly with V_g across V_g = 0. For a negative V_g, R is lowered with decreasing V_g, and it is enhanced for an opposite polarization of V_g. On the other hand, in Fig. 2(b), R changes

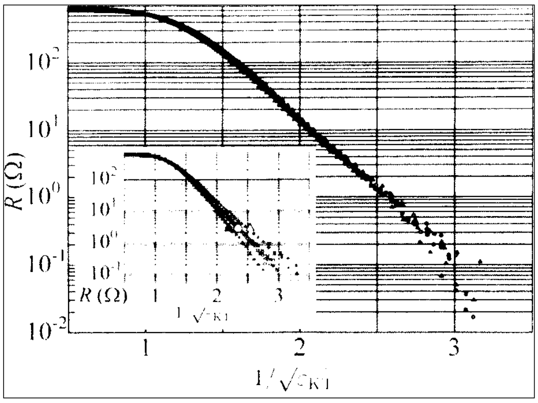

Figure 3. Temperature dependence of the resistance scaled in terms of ε_{KT} for a 2UCT YBCO film under zero magnetic field. The inset shows these in terms of ε_{KT0}. Symbols denote (O) V_g = 0, (Δ) V_g = 0.29V and (▲) V_g = -0.29V, respectively.

with V_g in a nonlinear fashion, that is, it approaches zero at a certain negative V_g and remains zero for a large negative V_g within an experimental error. This indicates that the onset temperature of zero resistance is altered by the applied E-field.

We analyzed the superconducting transition of ultrathin YBCO films by using the theory of Kosterlitz-Thouless (KT) transition. The superconducting part σ_S of the sheet conductance σ for the KT transition ig given by

$$\sigma_S = \sigma_N \exp\left(2(b\varepsilon_C/\varepsilon_{KT})^{1/2}\right) \qquad (1)$$

where σ_N and b are unknown parameters, $\varepsilon_C = (T_{mf} - T_{KT})/T_{KT}$, $\varepsilon_{KT} = (T - T_{KT})/T_{KT}$, T_{KT} is the transition tempertature of the KT transition, and T_{mf} is that of the mean-field transition, respectively. To evaluate T_{KT} we treated σ_N, $b\varepsilon_c$ and T_{KT} as fitting parameters and then the temperature was scaled to ε_{KT}. We obtain for T_{KT} 33.39K, 34.09K and 34.79K for V_g = +0.29V, 0V and -0.29V, respectively.

In Fig. 3, resistance curves under applied E-fields V_g = +0.29 V and V_g =0 are shown in respective scaling temperatures $1/(\varepsilon_{KT})^{1/2}$ based on eq. (1) where T_{KT} is chosen for each V_g. For scaling, R is shown against the scaling temperature $1/(\varepsilon_{KT0})^{1/2}$ for a fixed T_{KT} of V_g = 0 in the inset of Fig. 3. Here, the curves for V_g = +0.29V are separated by a straight line for V_g = 0 and deviate from each other at low temperatures. In contrast to this, they collapse into a unified function when scaling temperatures $1/(\varepsilon_{KT})^{1/2}$ are used for respective T_{KT}´s for each V_g.

We compare the E-field effects on T_{KT} with those on R_n and find that $\Delta T_{KT}/T_{KT}$ is proportional to $\Delta R/R_{n0}$ for various applied E fields. E-field effects study for other systems is in progress.

References

1. K. Kawahara, T. Suzuki, E. Komai, K. Nakazawa, T. Terashima and Y. Bando, Physica C, **266**, 149-156 (1996).
2. T. Kawahara, T. Suzuki, K. Shimura, T. Terashima and Y. Bando, Physica C, **235-240**, 3363-3364 (1994).